Biology of Reproduction, 2018, 99(2), 409–421
doi:10.1093/biolre/ioy042
Research Article
Advance Access Publication Date: 9 February 2018

OXFORD

Research Article

Human trophoblast epithelial-mesenchymal transition in abnormally invasive placenta†

Sonia C. DaSilva-Arnold[1], Stacy Zamudio[1], Abdulla Al-Khan[1], Jesus Alvarez-Perez[1], Ciaran Mannion[2], Christopher Koenig[2], Davlyn Luke[1], Anisha M. Perez[1], Margaret Petroff[3], Manuel Alvarez[1] and Nicholas P. Illsley[1,*]

[1]Department of Obstetrics and Gynecology, Hackensack University Medical Center, Hackensack, New Jersey, USA; [2]Department of Pathology, Hackensack University Medical Center, Hackensack, New Jersey, USA and [3]Department of Pathobiology and Diagnostic Investigation, College of Veterinary Medicine, Michigan State University, East Lansing, Michigan, USA

*__Correspondence__: Department of Obstetrics and Gynecology, Hackensack University Medical Center, 30 Prospect Ave, Hackensack, NJ 07601, USA. Tel: +551-996-8122; Fax: +551-996-8322; E-mail: nicholas.illsley@hackensackmeridian.org

†The datasets generated and analyzed during the current study are available in the GEO repository, accession number GSE104350.

Conference Presentation: Presented in part at the Society for Reproductive Investigation, March 2015, San Francisco, CA, and the International Federation of Placenta Associations, September 2015, Brisbane, Australia.
Edited by Dr. Peter J. Hansen, PhD, University of Florida.

Received 22 November 2017; Revised 5 January 2018; Accepted 7 February 2018

Abstract

Differentiation of first trimester human placental cytotrophoblast (CTB) from an anchorage-dependent epithelial phenotype into the mesenchymal-like invasive extravillous trophoblast (EVT) is crucial in the development of the maternal–fetal interface. We showed previously that differentiation of first trimester CTB to EVT involves an epithelial-mesenchymal transition (EMT). Here we compare the epithelial-mesenchymal characteristics of CTB and EVT derived from normal third trimester placenta or placenta previa versus abnormally invasive placenta (AIP). CTB and EVT were isolated from normal term placenta or placenta previa following Caesarean section and EVT from AIP following Caesarean hysterectomy. Cell identity was validated by measurement of cytokeratin-7 and HLA-G. Comparing normal term CTB with EVT from normal term placenta or placenta previa for differential expression analysis of genes associated with the EMT showed changes in >70% of the genes probed. While demonstrating a mesenchymal phenotype relative to CTB, many of the gene expression changes in third trimester EVT were reduced relative to the first trimester EVT. We suggest that third trimester EVT are in a more constrained, metastable state compared to first trimester equivalents. By contrast, EVT from AIP demonstrate characteristics that are more mesenchymal than normal third trimester EVT, placing them closer to first trimester EVT on the EMT spectrum, consistent with a more invasive phenotype.

Summary Sentence

Extravillous trophoblast cells from abnormally invasive placenta demonstrate more mesenchymal characteristics than normal third trimester cells, consistent with an overinvasive phenotype.

Key words: placenta, trophoblast, differentiation, accreta, abnormally invasive placenta, epithelial-mesenchymal transition.

Introduction

Abnormally invasive placenta (AIP; placenta accreta, increta, and percreta) occurs when trophoblast invasion progresses beyond the normal anchoring of the placenta to the uterine wall. Such overinvasion can be relatively shallow (accreta), deep into the myometrium (increta), or even through the uterine serosa (percreta). AIP can cause irreparable uterine damage and, in the worst cases, can invade into the bladder, bowel, pelvic sidewall, and other structures in the abdomen. Even with early diagnosis and expert clinical care, AIP can cause catastrophic blood loss at delivery. It is virtually always associated with maternal morbidity in the form of excess blood loss, and still carries a strong risk of mortality where diagnosis is absent prior to delivery, especially in low resource medical settings. The more severe forms of AIP require hysterectomy and frequently necessitate intricate surgical procedures to repair extrauterine damage [1, 2]. Trophoblast remodeling has been observed deep in the myometrial arteries in AIP, well beyond the normal spiral artery invasion [1, 3] and other pelvic blood vessels are often abnormally enlarged [4]. Thus, when removal of the adherent placenta is attempted, significant hemorrhage occurs because these deep arteries are of a larger caliber than the spiral arteries that are the normal focus of trophoblast invasion [3].

AIP is primarily an iatrogenic pathology. The major risk factors for AIP are implantation in the lower uterine segment, especially placenta previa (PP), and uterine scarring from procedures such as Caesarean section [5]; the two combined sharply increase risk. Increasing rates of Cesarean section have contributed to at least a 10-fold increase in AIP incidence, from 1:25 000 in the 1950s, to current rates as high as 1–2/1000 in the USA and Canada [6, 7]. Despite the rapidly increasing incidence, little is known of the molecular etiology. It is assumed that the epidemiological associations with PP and with uterine scarring are due to reduced resistance to trophoblast invasion. This more permissive environment is thought to be due to reduced thickness of the endo-myometrium around the cervix (in the case of PP), the presence of a noncellular pathway through the Caesarean scar, impaired decidual formation, or similar defects. There is only limited supporting evidence for these assumptions [8, 9]. It is apparent that other factors are involved, since many pregnancies with a PP and uterine scarring do not progress to AIP.

The question of what factor(s) might be driving at-risk pregnancies to AIP has garnered little attention, despite a vast literature on regulation of trophoblast invasion. There has also been a dearth of molecular analyses, with what little data have been reported relying on subjective methods like immunohistochemistry (IHC), and little attention paid to disease severity (accreta, increta, percreta). Wehrum et al. [10] observed the coexpression of cytokeratin-7 (an epithelial marker) and vimentin (a mesenchymal marker) in interstitial extravillous trophoblast (EVT) from placentas diagnosed histopathologically as abnormally invasive. They suggested that this was the consequence of a shift, in AIP, to a mesenchymal phenotype, characteristic of the epithelial-mesenchymal transition (EMT) observed in embryonic development, wound healing and in cancer metastasis [11, 12].

The EMT is a well-recognized phenomenon whereby epithelial cells differentiate into a mesenchymal phenotype and separate from the epithelium, enabling them to migrate away from the originating epithelial layer. Cytotrophoblast (CTB) at the tips of the villous columns attached to the maternal decidua undergoes a process resembling EMT as they differentiate into EVT and invade into the uterine lining. Support for EMT as part of the CTB to EVT differentiation process has been proposed by a number of laboratories, although this has been, for the most part, based on the expression of only two to three genes or proteins [13–17]. Using an 84-gene, PCR array we have shown that the comparison of first trimester CTB with first trimester EVT displays the gene expression characteristics of an EMT [18]. There are a number of marked differences with the processes described for the EMT in development, fibrosis, and metastasis that highlight trophoblast EMT as a different and unique type compared to other well-described varieties of EMT [11, 12]. We hypothesized that the mesenchymal characteristics we observed in first trimester EVT [18] would be retained in normal third trimester pregnancy but might reflect, at the molecular level, a more constrained, metastable phenotype. We also hypothesized that EVT from AIP would retain more of a first trimester-like phenotype, in which invasion into maternal tissues is most pronounced.

Placental research has been complicated by the use of placental homogenates for molecular studies, in which the relative ratios of specific cell types (trophoblast, endothelial, stromal, etc.) cannot be easily ascertained. We therefore devised methods to isolate EVT from third trimester tissues so as to be able to make direct and relevant comparisons in AIP versus controls. Before evaluating changes resulting from AIP, we first quantified the differences in gene expression between CTB and EVT from normal pregnancies. We compared CTB and EVT isolated from normal term placenta using a PCR array for genes known to be involved in EMT in other cell types. To control for the earlier gestational age at which AIP are delivered and for the relatively rare (1–3%) implantation of the placenta in the lower uterine segment, we additionally isolated control EVT from cases of PP (without AIP). In this disorder, the placenta lies over the cervical os, necessitating Caesarean delivery, often several weeks prior to term, due to bleeding. In order to maximize our ability to detect differences that may shed light on the molecular etiology of AIP, all pathological samples were derived from histopathologically confirmed cases of placenta percreta, the most severe form of AIP.

Materials and methods

Ethics

Human placental tissue for the preparation of trophoblast cells was obtained with written informed consent under approved protocols from Hackensack University Medical Center IRB and the Michigan State University IRB. Tissue acquisition and handling were carried out in accordance with relevant guidelines and regulations.

Subject selection

Control placentas for preparation of CTB (CTB-NT; normal term) and EVT (EVT-NT) were obtained from term (≥39 week) pregnancies without medical or obstetric complications and delivered by elective Caesarean section. Subjects in this group represent five healthy normal placentas from which CTB-NT were isolated and eight from which EVT-NT were prepared. Placenta previa was diagnosed by ultrasound, and tissue from PP pregnancies was obtained after delivery by elective Caesarean section. Placenta percreta (AIP) was diagnosed by ultrasound [19]. Delivery was by elective

Caesarean section followed immediately by hysterectomy. The diagnosis of placenta percreta was confirmed histopathologically by two experienced pathologists (CM, CK). All cases of placenta percreta were also PP. None of the previa or percreta pregnancies had other medical or obstetric complications.

Tissue sections

Basal plate tissue sections were obtained from normal placentae. Sections were embedded in 100% OCT compound (Tissue Tek, Torrance, CA) in cryomolds, frozen in liquid nitrogen and stored at –80°C until use.

EVT isolation

EVT were isolated from normal term placenta (EVT-NT) or placenta previa (EVT-PP) by removing a thin (2–3 mm) layer of tissue from the maternal-facing basal plate of the placenta immediately following delivery. Tissue (20 g) was washed 2× in phosphate-buffered saline (PBS), then further dissected into small pieces (2–4 mm) and washed 2× in PBS. EVT from AIP cases (EVT-AIP) were obtained from placental tissue obtained after hysterectomy. Following gross dissection of the uterus and adherent placenta, EVT-AIP were isolated from placental tissue taken from areas of deepest invasion, being careful to include the leading edge of abnormal invasion and adjacent areas. Where placental invasion had breached the uterine serosa, tissue was taken from the leading edge and adjacent to the area of the break-through. Placental tissue was dissected free of myometrium and uterine serosa, cut into small pieces (2–4 mm) and washed 2× in PBS. In all cases, tissue was maintained cold prior to dissection and placed in ice-cold PBS following dissection. Thereafter, tissue samples from NT, PP, and AIP pregnancies were treated in an identical manner.

Following dissection, placental tissue was incubated at 37°C in calcium- and magnesium-free Hank Balanced Salt Solution (HBSS) containing 10 mM Hepes, pH 7.4 with 0.05% trypsin (Thermo Scientific, Waltham, MA), 0.1% dispase (Worthington Biochemical, Lakewood, NJ), 0.01% DNAse I (Sigma-Aldrich, St Louis, MO). The tissue was incubated for 30 min and then the majority of the supernatant was decanted, through a 100-μm filter, into FBS (final concentration 10%) and placed on ice. Another aliquot of the digestion solution was added and the incubation, and filtration steps were repeated. Cells were pelleted by centrifugation (10 min, 1200 × *g*, 4°C) and resuspended in Separation Buffer (SB) which comprised calcium- and magnesium-free HBSS containing 2 mM EDTA, 0.5% BSA, pH 7.4. For all subsequent steps, cells were maintained at 4°C.

Resuspended cells were mixed with isotonic Percoll in SB to produce a final Percoll concentration of 20%. This mixture was layered on to a base layer of 60% Percoll and overlaid with 8% Percoll, then centrifuged in a fixed angle rotor (Sorvall SS-30) at 1200 × *g* for 30 min at 4°C. Following the spin, material at the 20%/60% interface was removed, passed serially through 70 and 40 μm filters and diluted 4× with SB before centrifugation at 1200 × *g* for 10 min. After resuspension in SB, cells were incubated with an anti-HLA-G antibody coupled to R-phycoerythrin (HLA-G-PE, 1:500, clone MEMG/9; Thermo Scientific; see Supplementary Table T5) for 20 min at 4°C on a rocker. Labeled cells were washed 2× in SB (400× *g*, 5 min), resuspended, counted and the volume was adjusted to give 10^7 cells/100 μL. Cells were incubated with anti-PE microbeads (10 μL microbeads/100 μL cells; Miltenyi, San Diego, CA) for 15 min at 4°C, washed with SB and resuspended in 1 mL SB. Positive selection of HLA-G-labeled cells was performed on an AutoMACS immunomagnetic cell separator using a double-column positive selection procedure as specified by the manufacturer. Cells were resuspended in SB, counted and used thereafter for measurements of purity and specificity and for the preparation of RNA.

CTB isolation

CTB-NT were isolated as described previously from normal, term placenta [20]. CTB-PP and CTB-AIP were isolated by a variation of the method described for EVT-AIP. After dissection and digestion of the tissue as described above, cells were made up in 8% Percoll, layered on to a cushion of 60% Percoll and overlaid with SB. Procedures were identical to the EVT-AIP preparation thereafter, except that cells were incubated with an antibody against integrin ß4, coupled to R-phycoerythrin (integrin ß4-PE, 1:500, clone 58XB4; BioLegend, San Diego, CA). Positive selection using the same AutoMACS procedure produced the CTB-AIP cell fraction.

Flow cytometry

The preparative fractions were tested for the content of HLA-G or integrin ß4 positive cells immediately after isolation using the fluorescence of the PE bound to the cells. Dead cell content was measured simultaneously following a 20-min incubation of the cell fractions with 30 nM Sytox Green (Thermo Scientific). To measure the cellular expression of CTB and EVT markers, fixed cells (5–10 × 10^4 cells/mL) were separately incubated with primary antibodies for 30 min at 4°C. These included antibodies against integrin α6 (FITC-labeled, clone GOH3, 3 μg/mL; Santa Cruz, Dallas, TX), and integrin α1 (Alexa 647-labeled, clone TS2/7, 2.5 μg/mL; AbD Serotec, Raleigh, NC). After washing in SB, labeled cells were analyzed by flow cytometry, using a Cytomics FC500 flow cytometer (Beckman-Coulter, Indianapolis, IN).

Cells were fixed for flow cytometry in order to measure intracellular components. Cells were pelleted (800 × *g*, 5 min), resuspended in 1% paraformaldehyde in 100 mM sodium phosphate, pH 7.4 and incubated for 15 min at room temperature. Cells were then pelleted, resuspended in PBS for storage at 4°C. Fixed cells were stained by incubation for 60 min at 4°C with anti-cytokeratin-7 (Alexa 488-labeled, clone EPR1619Y, 1 μg/mL; Abcam, Cambridge, MA), anti-vimentin (Alexa 488-labeled, clone RV202, 2.5 μg/mL; BD Biosciences, San Jose, CA) or anti-HLA-G (FITC-labeled, 1:200, clone MEM-G/9; Thermo Scientific).

RNA isolation and PCR array

Cells intended for PCR array experiments were pelleted immediately after isolation and extracted into buffer RLT (Qiagen, Valencia, CA) containing 40 mM DTT (0.8–1.6 × 10^6 cells/mL). RNA was prepared using the RNeasy Micro Kit (Qiagen) according to manufacturer's instructions. Following extraction, the concentration and integrity of the RNA was measured using an RNA 6000 Nano Kit on the Bioanalyzer 2100 (Agilent, Santa Clara, CA).

For the PCR array, 400 ng of RNA obtained from the various groups of cells was first reverse transcribed using the RT^2 First Strand cDNA Kit (Qiagen). The resultant cDNA was mixed with RT^2 SYBR Green Mastermix and equal aliquots were placed in the wells of a 96-well RT^2 Profiler PCR Array that contained a panel of 84 genes associated with the EMT (Cat. #PAHS090Z, Qiagen). The PCR Array was run on an ABI 7900 HT Fast Real-Time PCR System (Thermo Scientific) using the recommended cycling conditions.

Western blotting

CTB and EVT cell samples isolated as described above were washed 2× in PBS and extracted using a RIPA buffer. Samples (25 μg protein/well) were separated by 8–16% SDS-PAGE on a Criterion gel (Bio-Rad, Hercules, CA) and, following electrophoresis, proteins were transferred to nitrocellulose membranes using the Trans-Blot Turbo transfer system (Bio-Rad). Membranes were incubated overnight at 4°C with primary antibody, diluted in TBS (Tris-buffered saline) containing 3% BSA. The antibodies employed were rabbit polyclonal anti-cytokeratin-7 (1:1000; GeneTex, Irvine, CA), anti-matrix metalloproteinase-2 (MMP-2; 1:1000; GeneTex), anti-pleckstrin-2 (1:1000; Proteintech, Rosemont, IL), and anti-E-cadherin (1:2000; GeneTex), or mouse monoclonal anti-fibronectin (1:1000; clone 10/fibronectin, BD Transduction Laboratories), anti-occludin (1:1000; clone OC-3F10, Thermo Scientific), anti-HLA-G (1:500; clone MEM/G4, Thermo Scientific), anti-cytokeratin-14 (1:1000; clone LL002, Bio-Rad), anti-ß-actin (1:2000; clone AC15, Sigma-Aldrich), and anti-α-tubulin (1:2000; clone DM 1A, Sigma-Aldrich). After washing in TBST (TBS containing 0.1% Tween 20; 1 × 20 min, 2 × 10 min), membranes were incubated with anti-mouse or anti-rabbit IgG-HRP (1:20,000; Thermo Scientific) in TBS containing 3% BSA for 60 min at room temperature, then washed as before. Blots were visualized using the Trident Plus chemiluminescence kit (GeneTex) on a ChemiDoc MP imager (Bio-Rad) using the manufacturer's software (Image Lab). Blots were quantified using ImageJ64 (1.48v, NIH) and the bands were normalized to ß-actin or α-tubulin.

Fluorescent IHC

Tissue sections (5 μm) of term placentas were cut from OCT blocks and mounted onto positively charged slides. The tissue quality was verified by staining every 10th slide with H&E, and neighboring sections were fixed in ice-cold acetone or 1% paraformaldehyde (PFA) for 15 min, then washed 3× in PBS. PFA-fixed slides were permeabilized with 0.1% Tween-20 for 30 min, and washed 3× with PBS. Nonspecific binding was blocked with BlockAid (Thermo Scientific) for 1 h at room temperature. Immunolabeling was performed with mouse monoclonal anti-fibronectin Alexa Fluor 488 (1:100; clone FN3, eBioscience) and rabbit monoclonal anti-cytokeratin-7 Alexa Fluor 555 (1:250; clone EPR1619Y, Abcam) in a humidified chamber overnight at 4°C. Acetone-fixed slides were blocked against nonspecific binding in BlockAid for 1 h at room temperature. When higher background was observed (as in the case of HLA-G staining), immunolabeling was done in BlockAid containing 10% human AB serum (Cambrex, E. Rutherford, NJ). Colabeling with primary antibody was done in a humidified chamber overnight at 4°C; primary antibodies were comprised of rabbit monoclonal anti-cytokeratin-7 Alexa Fluor 488 (1:100; clone EPR1619Y, Abcam), mouse monoclonal anti-HLA-G (1:100; clone G233, Abcam), mouse monoclonal anti-occludin Alexa Fluor 488 (1:40; clone OC-3F10, Thermo Scientific), or rabbit polyclonal anti-E-Cadherin (1:100; GeneTex). Following incubation with primary antibodies, slides were washed 3× in PBS and incubated, where necessary, with fluorescent-dye conjugated secondary antibodies, including Alexa Fluor 555-labeled anti-mouse IgG or Alexa Fluor 488-labeled anti-rabbit IgG in BlockAid (1:500; Molecular Probes) for 30 min at room temperature and washed 3× with PBS. In all slides, the nuclei were counterstained with Hoechst 33342 (Molecular Probes) for 5 min at room temperature and washed 3× with PBS. Slides were air-dried and cover-slipped with ProLong Anti-Fade (Thermo Scientific). Images were acquired at the same exposure for all slides on a Zeiss Axioimager M1 epifluorescence microscope with an Axiocam 506 camera and merged with NIH Image J64 1.60v software.

Statistical analysis

Data normality was determined using the D'Agostino and Pearson normality test. Demographic and flow cytometry data were analyzed by one-way ANOVA using Tukey Multiple Comparison post hoc test. Sex- and gestational-age specific birthweight centiles were calculated according to Fenton and Kim [21]. The data from the PCR Array was analyzed using $\Delta\Delta C_T$ methodology to obtain the fold change in relative gene expression between different groups of cells. Combinations of five housekeeping genes (*B2M, GAPDH, ACTB, HPRT1, RPLP0*) were used to normalize our samples. Housekeeping genes demonstrated an absence of significant changes in C_T values across the sample groups ($P < 0.05$, unpaired *t*-test). The statistical significance of the gene expression differences between two groups was determined from the $2^{(-\Delta CT)}$ values using either an unpaired, two-tailed *t*-test or a two-tailed Mann–Whitney U-test, as appropriate. Western blotting data was compared using a two-tailed Mann–Whitney U-test. A P value of ≤ 0.05 was taken as indicating a significant difference. Data are presented as mean ± SEM unless otherwise stated.

Data availability

A full summary of the data generated during the current study is available in the Supplementary Information associated with the study. The datasets used to generate the gene expression information are available in the NCBI GEO repository, accession number GSE104350.

RESULTS

Demographic/clinical characteristics

There was no difference in maternal age (Table 1) between the normal term groups (CTB-NT, EVT-NT), the placenta previa group (CTB-PP, EVT-PP) and the AIP group (CTB-AIP, EVT-AIP). The EVT-AIP group was of higher gravidity and parity and had a greater number of prior Cesarean deliveries than the other groups. Gestational age at delivery was lower in the AIP groups than the NT groups (≥39 weeks). The gestational age at delivery of the PP groups did not differ from the AIP groups. Birth weight centiles normalized for gestational age and fetal sex did not differ between the groups. None of the pregnancies in the CTB-NT or EVT-NT groups had a PP. Deliveries for all groups were by elective, nonlaboring Cesarean section, and in the EVT-AIP group only, was followed by hysterectomy.

Cell isolation

The methodology for purification of EVT was developed using normal term placental tissue with the intention of subsequently applying it to the isolation of EVT from the placenta of AIP pregnancies. The only published isolation procedure for third trimester EVT utilized an overnight incubation step to separate non-adherent cells [22]. We therefore devised a new method to allow for rapid isolation of purified cells, minimizing any changes in gene expression due to significant incubation time in the *ex vivo* environment. We were able to test these procedures on AIP pregnancies during the course of methodological development. The tissue requirements for

Table 1. Demographic data.

Maternal characteristics

	N	Age	Gravidity	Parity	Prior C/S
CTB-NT	5	31.0 ± 2.3	3.4 ± 0.7	2.6 ± 0.4	1.2 ± 0.4
CTB-PP	3	31.7 ± 3.3	2.7 ± 0.3	1.0 ± 0.6	1.0 ± 0.6
CTB-AIP	3	32.0 ± 2.5	4.7 ± 1.2	2.7 ± 0.3	2.0 ± 0.6
EVT-NT	8	35.6 ± 1.0	2.9 ± 0.4	1.3 ± 0.2	1.3 ± 0.2
EVT-PP	8	33.5 ± 2.2	2.8 ± 0.6	1.1 ± 0.4	0.9 ± 0.3
EVT-AIP	8	36.1 ± 1.5	6.3 ± 1.3*	4.0 ± 0.9**	2.8 ± 0.3***

*Gravidity: EVT-AIP > EVT-PP, $P < 0.05$.
**Parity: EVT-AIP > EVT-NT, EVT-PP, $P < 0.05$.
***Prior C/S: EVT-AIP > CTB-NT, CTB-PP, CTB-AIP, EVT-NT, EVT-PP, $P < 0.05$.

Neonatal characteristics

	N	Gestational age	Birth weight	Birth weight centile
CTB-NT	5	39.2 ± 0.1	3564 ± 88**	82.8 ± 4.5
CTB-PP	3	35.8 ± 0.7	3066 ± 478	79.0 ± 10.0
CTB-AIP	3	34.1 ± 0.2	2417 ± 34	71.7 ± 3.2
EVT-NT	8	39.2 ± 0.1	3463 ± 149***	50.1 ± 10.2
EVT-PP	8	35.0 ± 1.2	2455 ± 225	47.6 ± 8.3
EVT-AIP	8	32.6 ± 0.6*	2335 ± 149	63.0 ± 7.6

*Gestational age: EVT-AIP < CTB-NT, EVT-NT, $P < 0.05$.
**Birth weight: CTB-NT > CTB-AIP, EVT-PP, EVT-AIP, $P < 0.05$.
***Birth weight: EVT- NT > CTB-AIP, EVT-PP, EVT-AIP, $P < 0.05$.

diagnostic histopathology and the goal of limiting tissue sampling to the leading edge of the overinvasion area in the EVT-AIP pregnancies meant that the quantity of the tissue available was limited. On average, we isolated 1–2 × 10^5 cells/g (EVT-NT, EVT-PP) from normal placentae but only 0.25–0.50 × 10^5 cells (EVT-AIP) from the tissue available from AIP cases.

We utilized the binding of PE-labeled anti-HLA-G as an index of EVT purity during the course of cell isolation for the various groups. The initial enzymatic digest of AIP tissue contained only 1.3 ± 0.3% HLA-G labeled cells (n = 8) compared to the 3.7 ± 0.8% in the NT digest (n = 8). The final fractions show much closer correspondence, with the EVT-AIP samples showing similar purity (85.5 ± 4.1%; EVT-AIP) to the EVT-PP (93.1 ± 1.9%) and the EVT-NT (97.2 ± 1.4%; Kruskal–Wallis, $P > 0.05$). Further data on the purification processes are shown in Supplementary Figure S1.

We isolated ~2 × 10^6 CTB/g from the tissue obtained from both PP pregnancies (CTB-PP) and AIP pregnancies (CTB-AIP). The binding of anti-integrin ß4-PE was used an index of purity for the CTB; CTB-PP and CTB-AIP were 98.6 ± 0.7% and 92.9 ± 4.3% integrin ß4-positive respectively (n = 3, 3).

CTB and EVT characteristics

To confirm the identity of the isolated cells, we analyzed subsets of fixed cells by flow cytometry. These measurements employed markers for trophoblast (cytokeratin 7), for mesenchymal cells (vimentin) and for EVT (HLA-G). In addition to the primary cells isolated from placental tissue, we used two cell lines, from human embryonic kidney (HEK293T) and early human placental choriocarcinoma (JEG3), as controls for the expression of vimentin (HEK293T) and for cytokeratin-7 and HLA-G (JEG3). The results show (Figure 1A), as expected, that the HEK293T show a high degree of staining for vimentin (93.0 ± 3.9%, n = 6) but minimal staining for cytokeratin-7 (3.0 ± 1.3%) and for HLA-G (0.2 ± 0.1%). JEG3 shows a high degree of staining for cytokeratin-7 (90.0 ± 2.2%, n = 8), a moderate degree of staining for HLA-G (44.8 ± 10.5%) and minimal staining for vimentin (2.8 ± 1.0%). CTB-NT demonstrate a high degree of cytokeratin-7 staining (94.5 ± 4.5%, n = 5) with no significant HLA-G staining (0.9 ± 0.4%) and minimal staining for vimentin (8.1 ± 3.2%). The EVT-NT showed both high degrees of staining for CK7 (97.6 ± 0.8%, n = 8) and HLA-G (93.5 ± 1.3%) with low vimentin staining (9.7 ± 3.4%). Similar staining results were shown for the other CTB and EVT groups (data not shown). These findings support the unique identity of the CTB (cytokeratin-7 positive, HLA-G negative, vimentin negative) and EVT (cytokeratin-7 positive, HLA-G positive, vimentin negative), as well as confirming a high degree of purity for the cell isolates. Notably, while a low expression of vimentin in CTB-NT was predicted, EVT-NT also demonstrated a low expression of vimentin.

As further confirmation of EVT identity, using flow cytometry we examined the "integrin switch," which has been described as a feature of the differentiation from the CTB to EVT phenotype [23–25]. This is characterized by the loss of integrin $\alpha 6$, normally observed in CTB (but not EVT), in conjunction with the acquisition of integrin $\alpha 1$, found in EVT but not CTB. CTB-NT and EVT-NT cells were stained for integrin $\alpha 6$ and integrin $\alpha 1$ immediately after isolation and the degree of staining was assessed by flow cytometry. JEG3 cells were stained as positive controls. Both JEG3 and CTB cells were positive for integrin $\alpha 6$ (75.3 ± 15.3, 89.7 ± 7.1%) and negative for integrin $\alpha 1$ (10.6 ± 7.2, 1.4 ± 0.9%; Figure 1B). EVT-NT showed minimal integrin $\alpha 6$ staining (4.3 ± 0.7%) and a high degree of positivity for integrin $\alpha 1$ (62.7 ± 5.9%). The integrin staining observed here shows the distinctive integrin switching in our purified cell fractions and confirms their identification as CTB and EVT.

PCR array

The RIN (RNA Integrity Number) score was used to assess the quality of the RNA extracted from isolated cells. The CTB-NT, CTB-PP,

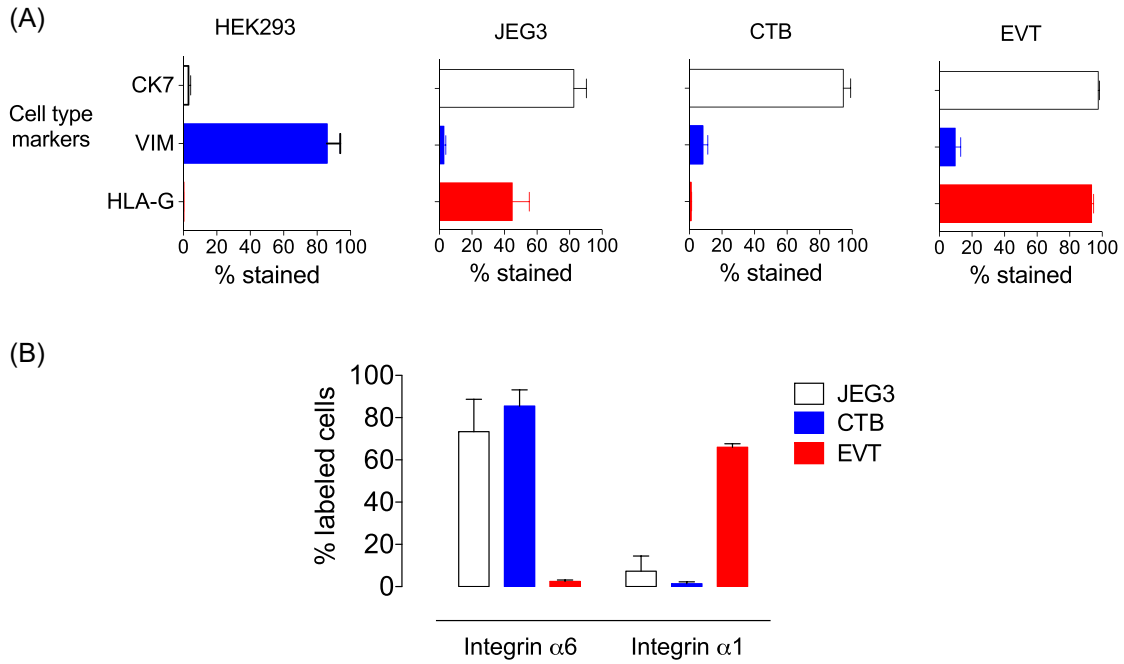

Figure 1. Characterization of CTB and EVT. (A) CTB and EVT purity: several different cell types were stained with fluorescent-labeled antibodies and staining was quantified by flow cytometry, including HEK293T (n = 8), JEG3 (n = 9), CTB-NT (n = 5), and EVT-NT (n = 8). Figure shows the percentage of cells in each cell type labeled by anti-cytokeratin 7-Alexa 488 (CK7), anti-vimentin-Alexa 488 (VIM), or anti-HLA-G-PE (HLA-G). (B) Integrin switching between trophoblast phenotypes: JEG3 (n = 8), CTB-NT (n = 5), and EVT-NT (n = 8) were labeled by antibodies to integrin α1 (integrin α1-Alexa 647) and integrin α6 (integrin α6-FITC), and the percentages of stained cells were quantified by flow cytometry.

and CTB-AIP had scores of 8.2 ± 0.2, 10.0, and 9.9 ± 0.1 (n = 5, 3, 4), while scores for the EVT-NT, EVT-PP, and EVT-AIP were 9.6 ± 0.1, 8.7 ± 0.4, and 9.3 ± 0.3, respectively (n = 8, 8, 8). This shows a high degree of RNA integrity for all samples, affirming their suitability for qPCR analysis. The PCR array comprised a panel of 84 genes associated with the EMT. The controls built into the PCR array showed that none of the samples had genomic DNA contamination and that the efficiency of both the reverse transcription and PCR were appropriate.

The PCR Array is composed of genes identified by the manufacturer from a variety of sources as being involved in an EMT (https://www.qiagen.com/us/shop/pcr/primer-sets/rt2-profiler-pcr-arrays/?catno=PAHS-090Z#geneglobe). We performed several comparisons of gene expression to assess the extent of EMT. Initially, we compared third trimester CTB-NT to the equivalent EVT-NT to assess normal third trimester EMT status. As the appropriate gestational age comparison for EVT-AIP gene expression is EVT-PP, we then compared EVT-PP to EVT-NT, to determine if there were any significant effects of gestational age on normal EVT. Following these, we compared EVT-AIP to EVT-PP to determine if EMT status was altered in the overinvasion pathology of AIP. Finally, we verified that the changes observed in EVT-AIP were not due to intrinsic alterations in CTB-AIP compared to CTB-PP.

CTB-NT and EVT-NT

The first gene expression comparison was between CTB-NT (n = 4) and EVT-NT from normal pregnancies (n = 8). Of the 84 genes associated with the EMT, 56 showed significant changes, with 31 upregulated and 25 downregulated (Supplementary Table T1). These changes involved many of the classical markers of the EMT, including the epithelial and mesenchymal markers, metalloproteinases, and transcription factors shown in Figure 2A. In EVT-NT, there is downregulation of a group of epithelial marker genes such as *CDH1* (E-Cadherin) and *EGFR* (EGF receptor), as well as other genes involved in epithelial junctional complexes (*OCLN*, occludin; *CTNNB1*, beta-catenin; *DSC2*, desmocollein 2; *DSP*, desmoplakin). There is corresponding upregulation of mesenchymal markers (*FN1*, fibronectin; *ITGA5*; integrin alpha 5; *ITGB1*, integrin beta 1). Surprisingly, expression of vimentin, a classical mesenchymal marker, was not altered. There are also prominent changes in the expression of proteases (*MMP2*, *MMP3*, *MMP9*, matrix metalloprotease 2, 3, 9; *BMP1*, bone morphogenetic protein 1) and their inhibitors (*TIMP1*, tissue inhibitor of metallopeptidase 1; *SERPINE1*, serpine family E member 1; *TFPI2*, tissue factor pathway inhibitor 2), although, interestingly, *MMP9* is down- rather than upregulated. There are also changes in the transcription factors described as master regulators of EMT, including *FOXC2* (forkhead box C2), *SNAI2* (snail family transcription repressor 2), *TWIST1* (twist family bHLH transcription factor 1), and *ZEB2* (zinc finger E-box binding homeobox 2). Of the 31 upregulated genes, 25 change in the direction consistent with EMT changes observed previously, while six change in the opposite direction. Of the 25 downregulated genes, 15 change in the direction predicted for EMT and 10 change in the opposite direction. Thus, a substantial majority of the gene expression changes (~70%) are consistent with an EMT, as described for other cell types, supporting the concept that an EMT is responsible for the gene expression differences seen between third trimester CTB-NT and EVT-NT.

We compared the extent of the EMT-associated gene expression changes to those which we previously reported for the first trimester [18]. While both the first and third trimester assessments demonstrated gene expression differences between CTB-NT and EVT-NT

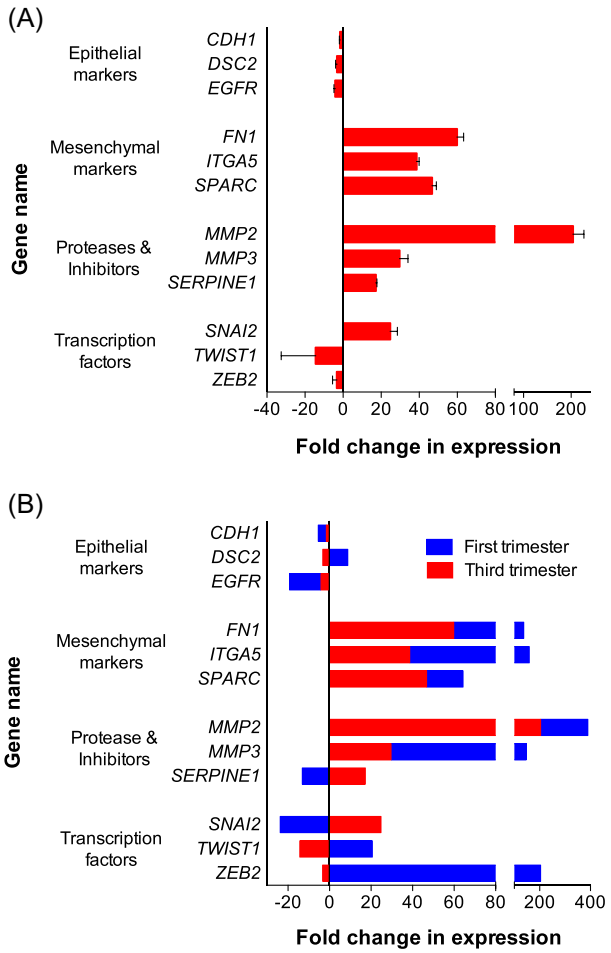

Figure 2. Differential EMT-associated gene expression in third trimester EVT. (A) This figure shows a selected subset of EMT-associated genes that demonstrate a significant ($P < 0.05$) alteration in third trimester EVT-NT (n = 8) compared to third trimester CTB-NT (n = 4). The fold-change in gene expression is shown as mean ± SEM for (a) junctional/epithelial marker genes, (b) genes encoding mesenchymal markers, (c) genes for matrix metalloproteinases and inhibitors, (d) genes encoding transcription factors. Full data are given in Supplementary Table T1. (B) For the same select groups of genes described in Figure 2A, this figure shows the comparison between CTB/EVT gene expression, measured as fold change, for first (blue) and third trimesters (red). First trimester data are taken from DaSilva-Arnold et al [18].

consistent with an EMT, the comparison showed that of the EMT-associated changes in first trimester CTB-NT/EVT-NT differentiation, 69% were reduced or even reversed compared to the first trimester. Thus, in Figure 2B the third trimester data from Figure 2A is reproduced for a subset of the array genes, where third trimester differential expression is compared to the equivalent first trimester comparison. While retaining EMT characteristics, the magnitude of the third trimester CTB/EVT-NT differential gene expression is diminished compared to the first trimester.

EVT-NT and EVT-PP

The second gene expression comparison we undertook was between EVT from normal pregnancies (EVT-NT, n = 8) and those from placenta previa pregnancies (EVT-PP, n = 8), delivered at a much earlier gestational age. We predicted that in the absence of abnormal invasion, these two groups would be very similar in gene expression, despite the difference in the gestational age at delivery (35 vs. ≥39 weeks, PP vs. NT). Only four significant differences were found between these groups. The matrix metalloproteinase *MMP2* and inhibitor *TIMP1* were lower in EVT-PP than EVT-NT (–4.4 ± 0.1 fold and –2.0 ± 0.3 fold). Expressions of *GEMIN2* (Gem Nuclear Organelle Associated Protein 2) and *TSPAN13* (Tetraspanin 13) were also lower in EVT-PP compared to EVT-NT (–1.53 ± 0.3, –1.5 ± 0.1 fold). Complete data for the EVT-NT/EVT-PP gene expression comparison is given in Supplementary Table T2. The presence of only four differences in gene expression out of 84 (two of which are less than a 2-fold change) led us to conclude that gene expression in the EVT-PP group differs minimally from the EVT-NT group, despite the 4-week difference in gestational age.

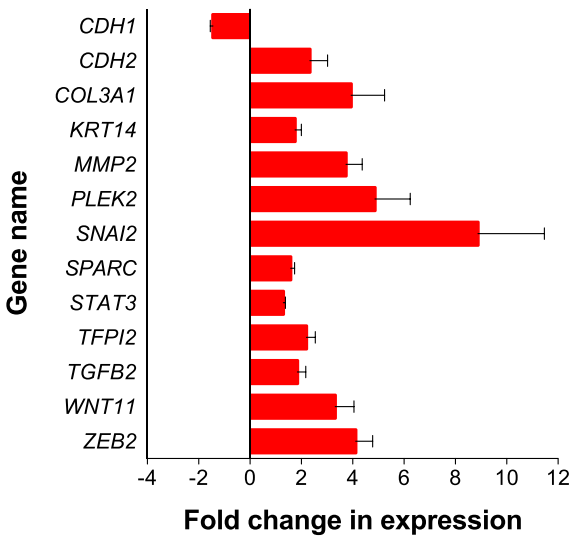

Figure 3. EMT-associated gene expression changes in EVT-AIP compared to EVT-PP. The figure shows the fold change in gene expression for those genes that demonstrate a significant ($P < 0.05$) change in expression in EVT-AIP (n = 8) compared to EVT-PP (n = 8). Full data are found in Supplementary Table T3.

EVT-PP and EVT-AIP

The third comparison was made between gene expression in EVT-PP (n = 8) and EVT-AIP (n = 8). Differential gene expression, over and above that occurring between CTB-NT and EVT-NT, occurred in 12 genes, all of which were upregulated except for *CDH1* (Figure 3). Many of these significant gene expression changes ((e.g., *CDH1*; *CDH2*, cadherin 2; *MMP2*; *PLEK2*, pleckstrin 2; *SNAI2*; *TGFB2*, transforming growth factor beta 2; *ZEB2*) are consistent with a further progression of the mesenchymal phenotype in the EVT-AIP versus EVT-PP or EVT-NT, as judged by changes occurring in other EMT types [12, 26–28]. Complete data on the EVT-PP/EVT-AIP gene expression comparison is given in Supplementary Table T3.

CTB-PP and CTB-AIP

It is possible that the differential expression between EVT-PP and EVT-AIP might have been a result of alterations in the precursor CTB, rather than changes in the differentiation process. We undertook, therefore, to compare CTB isolated from PP pregnancies (CTB-PP) with those isolated from AIP (CTB-AIP). PCR array results for comparison of CTB-PP (n = 3) with CTB-AIP (n = 3) showed no significant differences in gene expression across the full range of genes tested. Complete data on the CTB-PP/CTB-AIP gene expression comparison is given in Supplementary Table T4.

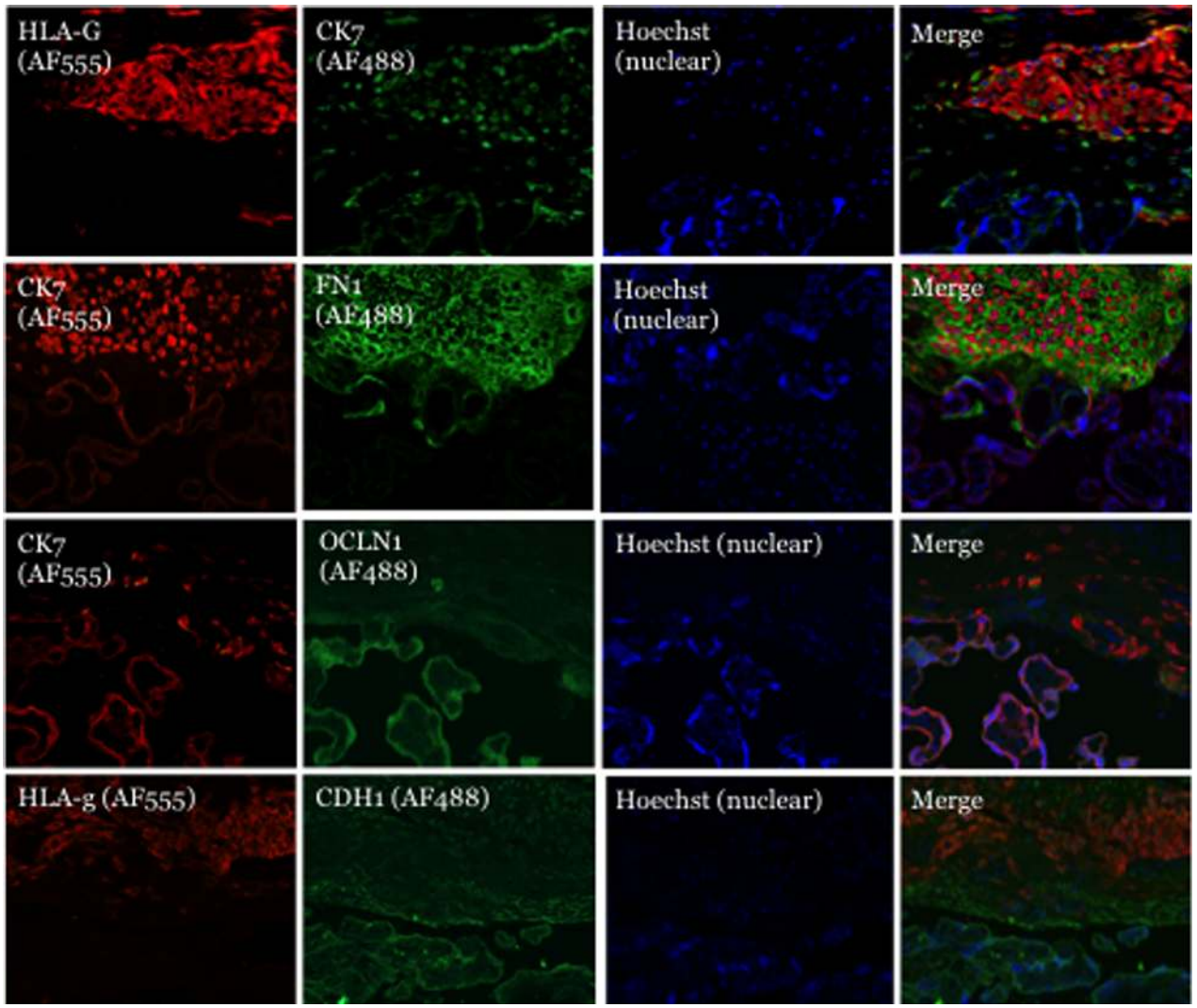

Figure 4. Comparison of CTB and EVT staining for markers and EMT-associated proteins in the basal plate of normal term placenta. (A) Staining for HLA-G (red), cytokeratin-7 (green), nuclei (blue), and the overlay of the three. (B) Staining for cytokeratin-7 (red), fibronectin (green) nuclei (blue), and the overlay of the three. (C) Staining for cytokeratin (red), occludin (green), nuclei (blue), and the overlay of the three. (D) Staining for cytokeratin (red), E-Cadherin (green), nuclei (blue), and the overlay of the three.

Protein validation

Using fluorescent IHC and western blotting, we investigated protein expression between CTB-NT and EVT-NT to show that key changes in gene expression are reflected in the production of the corresponding proteins. We were also able to perform western blotting to highlight some of the differences between EVT-PP and EVT-AIP. However, this was limited by the small quantity of cells available from the EVT-AIP. We chose not to compare EVT-NT and EVT-AIP by IHC, as the gene expression changes were relatively small and accurate IHC quantitation is extremely difficult under these circumstances.

Protein validation—fluorescent IHC

Sections of placental basal plate were incubated with antibodies against cytokeratin-7 and HLA-G to identify trophoblast and EVT cells, respectively, and the results from a representative example are shown in Figure 4. The top series of panels in Figure 4A shows the same section incubated with anti-HLA-G (red) and anti-cytokeratin-7 (green), Hoechst 33342 (blue) nuclear stain, and finally the overlay of all three. The HLA-G positive, cytokeratin-7 positive cells (EVT) in the basal plate region are clearly distinguishable from the HLA-G negative, cytokeratin-7 positive cells in the villous tissue (CTB, syncytiotrophoblast). Using these as a guide, we stained tissue sections for proteins for which a significant differential gene expression had been demonstrated between CTB and EVT. The next set of panels (Figure 4B) shows a section in which cytokeratin-7 (red) staining is apparent in both the villous tissue and basal plate. In the middle panel, staining for fibronectin (green), the gene for which (*FN1*) was upregulated 30-fold between CTB-NT and EVT-NT, is confined to the basal plate, while the merged panel shows EVT-NT embedded in the fibronectin. Figure 4C again shows cytokeratin-7 expression in both the villous and basal plate regions; however, the middle panel shows that occludin staining is primarily in the villous tissue with lower expression in the basal plate. This is consistent with the 63-fold decrease in *OCLN* expression between CTB-NT and EVT-NT. Figure 4D shows a section stained for cytokeratin-7 and E-cadherin, and

indicates a decrease between CTB-NT and EVT-NT, again tracking the 3-fold loss observed for *CDH1* gene expression. In summary, the fluorescent IHC data shows upregulation of HLA-G and fibronectin, in addition to the simultaneous loss of occludin and E-cadherin by the EVT, confirming that the differential gene expression is accompanied by parallel alterations in the corresponding proteins.

Protein validation—western blotting

A second method of protein validation, by western blot, was used to compare a series of proteins for which there were major differences in gene expression between CTB-NT and EVT-NT or between EVT-PP and EVT-AIP. Thus, we blotted CTB-NT and EVT-NT samples for cytokeratin-7, HLA-G, vimentin, fibronectin, MMP-2, occludin, and E-cadherin. Both CTB-NT and EVT-NT show strong expression of cytokeratin-7, but only the EVT-NT demonstrate the presence of HLA-G, while neither cell type exhibited significant quantities of vimentin (Supplementary Figure S2). The results for fibronectin and MMP-2 revealed substantial upregulation in EVT-NT compared to CTB-NT, paralleled by decreases in occludin and E-cadherin. These data were normalized ß-actin expression and the quantified data are shown in Figure 5A. The differences in protein expression mirror the changes in mRNA expression, with upregulation of HLA-G, fibronectin, and MMP-2 and downregulation of occludin and E-cadherin in EVT-NT. These results support that EVT-NT have a more mesenchymal phenotype than the CTB.

We blotted EVT-PP and EVT-AIP to compare expression of proteins for which the corresponding genes showed significant changes, including cytokeratin-14, MMP-2, and pleckstrin-2. We also examined the expression of cytokeratin-7 and HLA-G. The western blots are shown in Supplementary Figure S3 for cytokeratin-7, cytokeratin-14, HLA-G, MMP-2, and pleckstrin-2. These data were normalized to α-tubulin expression, and the quantified data are shown in Figure 5B. Expression of cytokeratin-7 and cytokeratin-14 was unchanged. Although these data do not show significant changes in the expression of MMP-2 and pleckstrin-2 in the EVT-AIP compared to the EVT-NT, there was a trend towards changes that parallel those in gene expression. In addition, there was a trend towards a decrease in HLA-G.

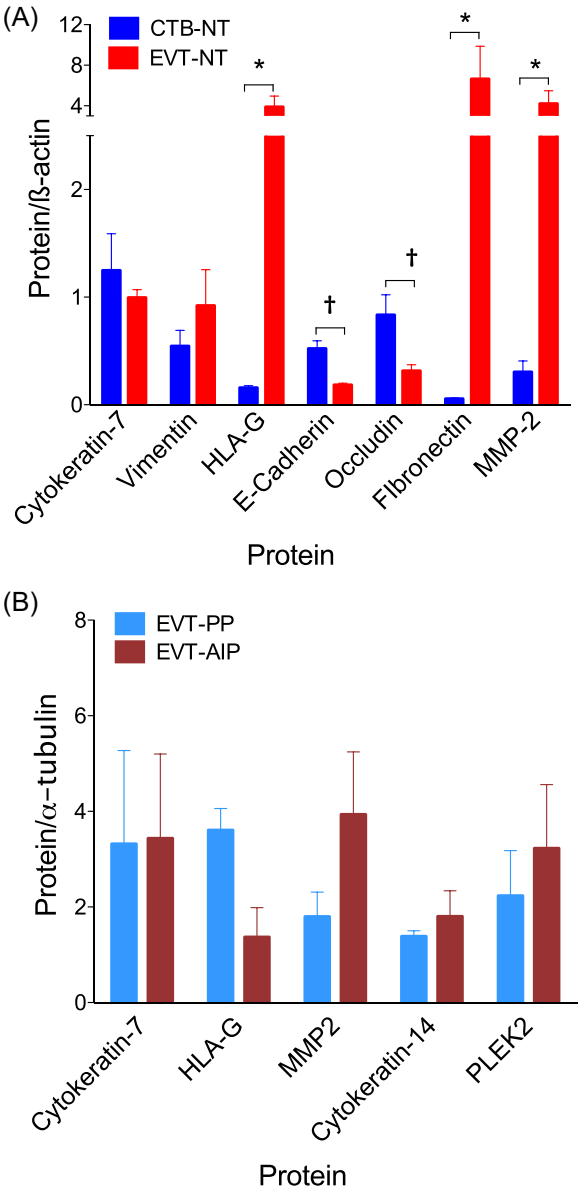

Figure 5. Western blotting for EMT-associated proteins. Proteins from three CTB-NT samples and three EVT-NT samples were separated by SDS-PAGE and transferred to nitrocellulose membranes. Membranes were blotted with antibodies against multiple antibodies as described in *Methods*. Chemiluminescence was measured using a ChemiDoc MP imager and bands were digitized using ImageJ64. (A) Comparison between protein expression in CTB-NT (blue) and EVT-NT (red). Protein expression was normalized to ß-actin expression from the same gel. *indicates where EVT-NT expression is greater than that in CTB-NT ($P < 0.05$). † indicates that CTB-NT protein expression is greater than EVT-NT ($P < 0.05$). Blot data are shown in Supplementary Figure S2. (B) Comparison between protein expression in EVT-PP (light blue) and EVT-AIP (magenta). Protein expression was normalized to α-tubulin expression from the same gel. Blot data are shown in Supplementary Figure S3.

DISCUSSION

We report here on our development of a novel protocol to rapidly isolate EVT from normal term and abnormally invasive human placenta and the subsequent comparison of EMT-associated gene expression between cells from control and AIP pregnancies. Cells were isolated from the placenta of third trimester pregnancies and, using a series of specific markers, we confirmed the identity of the cells as EVT by flow cytometry, IHC, and western blot. We then examined the up- or downregulation of specific EMT-associated mRNAs by PCR array. The profile of differential gene expression between third trimester CTB-NT and EVT-NT confirms our report of first trimester CTB to EVT transition [18]; of the genes showing a significant change in the third trimester comparison, approximately 70% are altered in a way that would be expected of an EMT, indicating that EVT acquire a mesenchymal phenotype as a result of the EMT.

Despite the maintenance of a more mesenchymal phenotype compared to CTB, third trimester EMT-associated gene expression in EVT-NT is clearly diminished compared to the first trimester. This is apparent in Figure 2B, which shows a reduction in the CTB/EVT gene expression changes between first and third trimesters. Over the entire array, of those genes that showed significant alterations between CTB and EVT in the first trimester, 74% showed a similar but diminished change in expression in the third trimester; e.g., *CDH1* expression, which was reduced by 10.8-fold in first trimester EVT (compared to first trimester CTB), was reduced by only 1.5-fold in third trimester EVT compared to third trimester CTB. Another

20% demonstrated a greater degree of change in the third trimester comparison and the remainder showed no difference between third trimester and first trimester. This leads us to conclude that the EVT-NT are in a metastable, and likely less active state, as described previously for both trophoblast and other cell types [29, 30]. We conclude that the third trimester EVT show signs of an EMT, despite the fact that some genes show no changes or changes opposite to those expected of an EMT. Some contrary changes in gene expression are to be expected. For example, there are substantial differences between the three defined types of EMT; however, simply because the gene expression changes in metastasis are not a replicate of those in gastrulation, for example, does not invalidate the metastatic EMT. The occurrence of an EMT can be judged by multiple characteristics including gene and protein expression. The CTB/EVT differentiation process demonstrates loss of cell-cell junctions, alterations in cell polarity, changes in invasive capacity and morphology as well as EMT-associated changes in gene and protein expression. As importantly, the CTB/EVT changes are being judged on the basis of the EMT process in other cell types and under very different conditions, circumstances that may not apply in this instance. For example, while *TWIST1* is categorized as an EMT master regulator and is upregulated in other forms of EMT, there is good evidence to show that in trophoblast *TWIST1* is centrally involved in syncytialization, the alternate CTB differentiation path [31, 32].

The EVT isolated in the manner described here may include those that are dispersed as interstitial EVT [33, 34] and, potentially, endovascular EVT. We attempted during tissue dissection to exclude larger blood vessels. Nonetheless, it is possible that the cell populations contained EVT subtypes, including endovascular EVT. It is also possible that the EVT collected from the basal plate may not be reflective of interstitial EVT found deeper into the decidua/myometrium. It is possible that the cell types in the basal plate will differ in gene expression, reflecting intermediate phenotypes characteristic of cells at various stages of the EMT. Despite this, the highly significant differences between CTB-NT and EVT-NT in the vast majority of the EMT-associated genes suggest that either the EVT isolated were predominantly of one type, or that the differences in the EMT-associated genes are common to all EVT types. Finally, it is possible that gene expression is modified during the cell isolation; however, apart from the digestion step, all procedures were carried out at 4°C, minimizing the possibility of transcriptional changes.

The differential gene expression profile obtained in the third trimester CTB-NT versus EVT-NT comparison is similar to those we recently reported for the first trimester [18]. Of the 56 differentially expressed genes in the third trimester comparison, 34 genes showed changes similar to those in the first trimester, supporting the contention that the differentiation process transforming CTB to EVT involves an EMT.

Despite the similarity between the first and third trimester comparisons, there is evidence to suggest that the highly active EMT process we reported in the first trimester is scaled back in the third trimester. There were 42 genes for which the degree of differential expression seen in the first trimester was significantly reduced in the third trimester, or in which differential expression was actually reversed (e.g., going from a positive, upregulation to a negative, downregulation) in the third trimester (Figure 2B). Thus, the first trimester CTB versus EVT comparison shows substantial downregulation of junctional epithelial genes, such as *CDH1* (E-cadherin; 7-fold) and *EGFR* (epidermal growth factor receptor; 24-fold), while in the third trimester the same genes show much more limited changes relative to CTB (*CDH1*, 1.5-fold; *EGFR*, 4-fold). Mesenchymal markers show

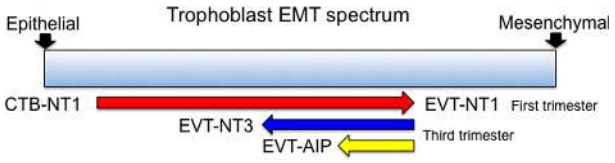

Figure 6. Diagram indicating cellular localization on the EMT spectrum. This diagram shows the EMT spectrum from the epithelial genotype on the left to the mesenchymal on the right. First trimester CTB (CTB-NT1) differentiate (red arrow) into first trimester EVT (EVT-NT1), traversing a major part of the spectrum but not becoming fully mesenchymal. Over the course of gestation, the extent of EMT-associated gene expression is reduced (blue arrow), moving towards the epithelial end of the spectrum and resulting in third trimester EVT (EVT-NT3, identical to EVT-PP). In AIP, however, the diminution of EMT-associated gene expression (yellow arrow) is not as marked as that seen in normal pregnancies, with EVT-AIP remaining in a more mesenchymal state compared to EVT-NT3.

a similar pattern; for example, in the first trimester there is upregulation of *FN1* (fibronectin; 107-fold), *ITGA5* (integrin $\alpha 5$; 140-fold), and *VIM* (vimentin; 235-fold) that was diminished in the third trimester (*FN1*, 60-fold; *ITGA5*, 39-fold; *VIM*, no change). We suggest that this is evidence that EVT obtained from the third trimester tissue, while still displaying features of the EMT process, may be less dynamic and have regressed towards a more epithelial position on the EMT spectrum compared to first trimester EVT (Figure 6). This is also apparent for several of the transcription factors assayed, including *SNAI2* and *ZEB2*. The latter, identified as an EMT "master regulator" [35, 36], is almost 200-fold higher in first trimester EVT compared to CTB and hence is a primary candidate for mediation of the differentiation-associated EMT process in early pregnancy. By contrast, third trimester expression of *ZEB2* is decreased (3.3-fold) in the EVT-NT compared to CTB-NT. The changes in epithelial and mesenchymal markers, matrix metalloproteinases, and transcription factors support that third trimester EVT are in what has been referred to in prior literature as a "metastable" state [29]. It is thought that EMT progression consists of the loss of epithelial characteristics simultaneous with the acquisition of mesenchymal features, such that elements of the two states can coexist in a "partial" EMT [16, 30]. In view of the plasticity demonstrated by the reverse, mesenchymal-epithelial transition (MET) [28, 30], "metastable" in this context means retention of the potential to progress either towards a mesenchymal state or to regress towards the epithelial state. This plasticity may enable EVT in the third trimester to revert to a less active form compared to the first trimester EVT, likely as a result of changes in the local environment and/or loss of stimulatory factors and consistent, in normal pregnancies, with the absence of the need for continued invasion.

During embryonic development, the most relevant type of EMT (type 1, developmental) plays a critical role in generating the first set of mesenchymal cells, known as the primary mesenchyme. Subsequently, as tissues expand and lineage specifications emerge, primary mesenchyme gives rise to secondary epithelia via the reverse process, MET [11, 27]. Several groups looking at one or more marker genes/proteins have suggested that the CTB differentiation process involves an EMT [13–17]. Of prior studies pointing to an EMT-like process in trophoblastic differentiation, the work by Knöfler et al. indicated changes in six EMT biomarkers in their comparison of first trimester CTB and EVT [17]. Many of the changes they observed are concordant with both the first and third trimester changes we have demonstrated in the present study and our prior report [18]. However, while sharing many features with type 1 EMT [11,

12], CTB/EVT differentiation differs significantly. CTB differentiation does not generate the mesenchyme of a new tissue, nor do the differentiated cells (EVT) undergo migration and a subsequent MET to generate a new epithelium. This is also reflected in differences at the molecular level. For example, the *TWIST1* and *FOXC2* transcription factors are upregulated in developmental EMT [26], but we showed that both are downregulated in first trimester CTB/EVT differentiation [18], and they show no change in third trimester EVT-NT compared to CTB-NT. *TWIST1* downregulation is supported by evidence showing that it is involved in the other pathway of CTB differentiation, syncytialization [31, 32]. As another example, developmental type 1 EMT involves loss of the epithelial cytokeratins [12]. However, CTB differentiation to EVT shows increased expression of cytokeratins [18, 29], in both first and third trimesters. The coexpression of mesenchymal and epithelial genes may be a means of maintaining the metastable, quasiepithelial status of EVT to ensure that, despite cell cycle exit and differentiation, invasion is limited by decidual constraints on the EMT. The EMT which drives CTB/EVT differentiation, while sharing characteristics with both developmental EMT and the other classical forms of EMT, displays a number of characteristics which mark it as a separate, fourth type of EMT.

Most previous reports which have suggested an EMT as the mechanism for CTB/EVT differentiation have been based on the analysis of a relatively small number of genes [10, 13–15, 17]. We sought to provide a more definitive conclusion, using a commercial PCR array containing 84 EMT-associated genes, chosen primarily from the EMT described in both metastasis and development. While this is an order of magnitude better than previous studies, some of the genes analyzed show no changes and it is probable than many genes that are significant in trophoblast EMT have not been defined. Further analysis of gene expression by methods such as RNA sequencing will enable us to confirm and describe the nature of the EMT governing CTB/EVT differentiation.

The protein validation studies support the identification of the difference between the CTB-NT and EVT-NT as the result of an EMT process. CTB-NT and EVT-NT are identified by the combination of cytokeratin-7 and HLA-G staining in the basal membrane sections. The loss of occludin and E-cadherin mirrors both the gene expression and immunoblot measurements. The increased staining for fibronectin in EVT-NT is readily apparent in both the immunohistochemical and western blot measurements, as is the change in MMP-2 in blotting experiments with CTB-NT and EVT-NT. Combined, the flow cytometric measures of the integrin $\alpha 6$/integrin $\alpha 1$ switch and the IHC and western blot changes are a clear indication that the changes in gene expression are accompanied by parallel alterations in the corresponding proteins, supporting EMT as the process governing CTB differentiation to EVT. Although there are no significant changes in proteins between EVT-AIP and EVT-PP, there is a trend in the protein expression of MMP-2 and pleckstrin-2 towards changes that parallel the alterations in gene expression, while the HLA-G shows a trend towards a decrease in expression.

In making the comparison between EVT derived from normal and pathological pregnancies, one important difference between the EVT-NT and the EVT-AIP is the gestational age at which each cell population was isolated. EVT-AIP cells were isolated prior to term and so comparison with EVT-NT might raise the question of whether the gestational age was responsible for any differences. We therefore isolated EVT-PP from PP pregnancies for comparison with EVT-AIP to control for the impact of earlier delivery and placental location within the uterus of the AIP pregnancies, since they were all also PP. We used PP as the control because it is likely that these pregnancies are closer to normal than other preterm births. The issue driving delivery is a mechanical one, blockage of the birth canal, rather than endocrine, metabolic, or other biochemical causes, which will have consequences for gene and protein expression. We compared the EVT-AIP isolated at 32.6 ± 0.6 weeks gestational age with EVT-PP, isolated at 34.9 ± 1.9 weeks, eliminating gestational age and implantation location as driving factors for any changes seen in EVT-AIP. The differences between EVT-PP and EVT-AIP, in terms of gene expression, indicate a more mesenchymal phenotype in EVT from AIP compared to PP.

The decrease in *CDH1* in EVT-AIP compared to EVT-PP may have effects broader than solely on cell adhesion functions. Knockdown of *CDH1* has been shown to cause increased invasiveness, increased expression of mesenchymal markers, upregulation of transcription factors and other features of EMT [37, 38]. Its further reduction in AIP is another indicator of a prolonged or extended EMT process. Changes in the proteins coded by *CDH1* (E-cadherin) and *MMP2* (MMP-2) have been noted previously in AIP [39, 40], supporting the changes we see here. In addition to the loss of *CDH1*, several other EMT-related processes are apparent in the gene expression changes attributable to AIP. These include continued cytoskeletal rearrangements marked by increased *KRT14* (keratin 14) and *PLEK2* gene expression and the augmented proteolytic capacity, shown by the increased expression of *MMP2*. Including these genes, nine genes (*CDH1*; *KRT14*; *MMP2*; *PLEK2*; *STAT3*, signal transducer and activator or transcription 3; *TFPI2*; *TGFB2*; *WNT11*, Wnt family member 11; *ZEB2*) show changes that place them closer on the EMT spectrum to first trimester EVT than those found in EVT-PP (Figure 6), consistent with the increased invasiveness characteristic of this pathology.

The other set of control experiments were designed to examine the possibility that the changes in gene expression between EVT-PP and EVT-AIP were a result of alterations in the precursor CTB, rather than changes in the differentiation process. We compared CTB from PP pregnancies with those obtained from AIP pregnancies. There were no significant differences in gene expression between the CTB-PP and CTB-AIP. The conclusion we draw from these data is that the changes in gene expression between EVT-PP and EVT-AIP stem from alterations in the differentiation process and not from differences in the precursor CTB.

There is likely a degree of heterogeneity within the EVT-AIP group. While all cases were histopathologically confirmed as placenta percreta, disease progression over the course of pregnancy is unknown. We do not know whether the trophoblast overinvasion characteristic of this pathology dates back to defects in the initial placental implantation, is stimulated at a later point in gestation, and to what degree the disease is progressive. It is unknown whether overinvasion is continuous and parallels growth of the placenta, or whether overinvasion occurs during a discrete, contained period. We anticipate being able to address this issue with new methods for the accurate imaging of AIP over gestation [19]. It is possible that any heterogeneity, beyond normal human genetic variation, may have obscured other changes.

As we have noted from a previous study and in the discussion above, while CTB/EVT differentiation in the first trimester demonstrates substantial molecular and phenotypic changes from an epithelial to a mesenchymal profile, the EVT still retains some epithelial features, such as cytokeratin expression, characteristic of a metastable state [18], and thus should not be considered fully mesenchymal. The differential gene expression shown between EVT-PP and EVT-AIP places the latter closer to the mesenchymal end of the

EMT spectrum than EVT-PP or EVT-NT, closer to the changes seen in the first trimester CTB/EVT comparison. We interpret this to mean that the regression in EMT status over gestation, as observed in third trimester EVT-NT, is not as pronounced in EVT-AIP (Figure 6). This would be compatible with the increased invasiveness characteristic of AIP. The cause of the diminished EMT status of EVT in the third trimester is not clear; it is very possible that the extent of EMT-associated changes is completely dependent on the uterine cellular environment, although intrinsic effects are also possible.

ZEB2 is one of the genes altered in EVT-AIP. The substantial increase in *ZEB2* in first trimester EVT, the reduction in third trimester EVT-NT (and EVT-PP), but increase in EVT-AIP are consistent with the action of *ZEB2* as an EMT master regulator in trophoblast differentiation. The absence of changes in the other master regulatory transcription factors (i.e., *FOXC2*; *GSC*, goosecoid; *SNAI1*, snail family transcriptional repressor 1; *SNAI2*; *TWIST1*) corresponding to the alterations in EVT invasiveness *in vivo* also supports the role of *ZEB2* as the intracellular factor controlling trophoblast EMT. Verification of this will require manipulation of trophoblast *ZEB2* expression in parallel with measures of invasiveness.

Ideally, the characterization of the EVT here would include relative measures of invasiveness as the functional correlate of the gene and protein expression studies. Unfortunately, the small number of cells available from the AIP samples has thus far precluded invasion assays in addition to the measures of gene and protein expression described here. We know, from the localization of the tissue from which the EVT-AIP were derived, that these cells are much more deeply invasive than those from control pregnancies. The establishment of the identity and characterization of these cells will enable us to use future AIP preparations to quantify the invasive capacity of the EVT-AIP.

Supplementary data

Supplementary data are available at *BIOLRE* online.

Supplementary Figure S1. EVT enrichment during preparation. The percentage of HLA-G-PE labeled cells at various stages of the EVT isolation from normal pregnancies (EVT; n = 21), pregnancies with a placenta previa (EVT-PP; n = 6), and with AIP (EVT-AIP; n = 14). The extent of HLA-G-PE labeling was measured by flow cytometry.
Supplementary Figure S2. Western blot of CTB-NT and EVT-NT. This figure shows data from two separate western blots for markers of EMT. In each blot, there are three CTB-NT samples and three EVT-NT samples, each isolated from a separate, normal third trimester placenta. Each blot shows the expression of ß-actin in the samples and used to normalize the expression of the proteins being investigated experimentally. The upper blot shows bands for fibronectin, E-cadherin, and cytokeratin-7. The lower blot shows bands for MMP-2 and vimentin. The data for the quantified blots are shown in Figure 5A.
Supplementary Figure S3. Western blot of EVT-PP and EVT-AIP. This figure shows data from two separate western blots for markers of EMT. In each blot, there are three EVT-PP samples and three EVT-AIP samples, each isolated from a separate, normal third trimester placenta. Each blot shows the expression of α-tubulin in the samples and used to normalize the expression of the proteins being investigated experimentally. The upper blot shows bands for cytokeratin-14, cytokeratin-7, and HLA-G. The lower blot shows bands for MMP-2 and pleckstrin-2. The data for the quantified blots are shown in Figure 5B.
Supplementary Table T1. Fold change in EVT-NT gene expression compared to CTB-NT.
Supplementary Table T2. Fold change in EVT-PP gene expression compared to EVT-NT.
Supplementary Table T3. Fold change in EVT-AIP gene expression compared to EVT-PP.
Supplementary Table T4. Fold change in CTB-AIP gene expression compared to CTB-PP.
Supplementary Table T5. Antibody Table.

Acknowledgments

The authors would like to acknowledge the assistance of their clinical obstetrical colleagues at Hackensack University Medical Center who helped in the acquisition of the clinical samples. The authors also thank Estela Bevilaqua, PhD, and her laboratory staff for sharing the EVT isolation technique initially developed in her laboratory.

Authors' contributions: Experiments were conceived and designed by SDA, NPI, SZ, and AA. AA, JAP, and MA were responsible for tissue acquisition and clinical data acquisition, review, and interpretation. CM and CK carried out the histopathological analyses. SDA, SZ, DL, AP, and NPI performed the experimental analyses and data collection. MP contributed materials. SDA, SZ, and NPI carried out the data interpretation. Manuscript was written by NPI and edited by SDA, SZ, MP, AA, and CM. Manuscript was approved for submission by all authors.

Conflict of Interest: The authors have declared that no conflict of interest exists.

References

1. Khong T. The pathology of placenta accreta, a worldwide epidemic. *J Clin Path* 2008; **61**:1243–1246.
2. Mazouni C, Gorincour G, Juhan V, Bretelle F. Placenta accreta: a review of current advances in prenatal diagnosis. *Placenta* 2007; **28**:599–603.
3. Tantbirojn P, Crum CP, Parast MM. Pathophysiology of placenta creta: the role of decidua and extravillous trophoblast. *Placenta* 2008; **29**:639–645.
4. Al-Khan A, Gupta V, Illsley NP, Mannion C, Koenig C, Bogomol A, Alvarez M, Zamudio S. Maternal and fetal outcomes in placenta accreta after institution of team-managed care. *Reprod Sci* 2014; **21**:761–771.
5. Publications Committee SfM-FM, Belfort MA. Placenta accreta. *Am J Obstet Gynecol* 2010; **203**:430–439.
6. Mehrabadi A, Hutcheon JA, Liu S, Bartholomew S, Kramer MS, Liston RM, Joseph KS, Maternal Health Study Group of Canadian Perinatal Surveillance S. Contribution of placenta accreta to the incidence of postpartum hemorrhage and severe postpartum hemorrhage. *Obstet Gynecol* 2015; **125**:814–821.
7. ACOG. ACOG Committee opinion. Number 529, July 2012: placenta accreta. *Obstet Gynecol* 2012; **120**:207–211.
8. Beuker JM, Erwich JJ, Khong TY. Is endomyometrial injury during termination of pregnancy or curettage following miscarriage the precursor to placenta accreta? *J Clin Pathol* 2005; **58**:273–275.
9. Garmi G, Goldman S, Shalev E, Salim R. The effects of decidual injury on the invasion potential of trophoblastic cells. *Obstet Gynecol* 2011; **117**:55–59.
10. Wehrum MJ, Buhimschi IA, Salafia C, Thung S, Bahtiyar MO, Werner EF, Campbell KH, Laky C, Sfakianaki AK, Zhao G, Funai EF, Buhimschi CS. Accreta complicating complete placenta previa is characterized by reduced systemic levels of vascular endothelial growth factor and by epithelial-to-mesenchymal transition of the invasive trophoblast. *Am J Obstet Gynecol* 2011; **204**:411.e1–411.e11.
11. Kalluri R, Weinberg RA. The basics of epithelial-mesenchymal transition. *J Clin Invest* 2009; **119**:1420–1428.
12. Zeisberg M, Neilson EG. Biomarkers for epithelial-mesenchymal transitions. *J Clin Invest* 2009; **119**:1429–1437.

13. Vicovac L, Aplin JD. Epithelial-mesenchymal transition during trophoblast differentiation. *Acta Anat (Basel)* 1996; **156**:202–216.
14. Floridon C, Nielsen O, Holund B, Sunde L, Westergaard JG, Thomsen SG, Teisner B. Localization of E-cadherin in villous, extravillous and vascular trophoblasts during intrauterine, ectopic and molar pregnancy. *Mol Hum Reprod* 2000; **6**:943–950.
15. Kokkinos MI, Murthi P, Wafai R, Thompson EW, Newgreen DF. Cadherins in the human placenta – epithelial-mesenchymal transition (EMT) and placental development. *Placenta* 2010; **31**:747–755.
16. Jordan NV, Johnson GL, Abell AN. Tracking the intermediate stages of epithelial-mesenchymal transition in epithelial stem cells and cancer. *Cell Cycle* 2011; **10**:2865–2873.
17. Knofler M, Pollheimer J. Human placental trophoblast invasion and differentiation: a particular focus on Wnt signaling. *Front Genet* 2013; **4**: 1–14.
18. DaSilva-Arnold S, James JL, Al-Khan A, Zamudio S, Illsley NP. Differentiation of first trimester cytotrophoblast to extravillous trophoblast involves an epithelial-mesenchymal transition. *Placenta* 2015; **36**:1412–1418.
19. Collins SL, Stevenson GN, Al-Khan A, Illsley NP, Impey L, Pappas L, Zamudio S. Three-dimensional power Doppler ultrasonography for diagnosing abnormally invasive placenta and quantifying the risk. *Obstet Gynecol* 2015; **126**:645–653.
20. Petroff MG, Phillips TA, Ka H, Pace JL, Hunt JS. Isolation and culture of term human trophoblast cells. *Methods Mol Med* 2006; **121**:203–217.
21. Fenton TR, Kim JH. A systematic review and meta-analysis to revise the Fenton growth chart for preterm infants. *BMC Pediatr* 2013; **13**:59.
22. Borbely AU, Sandri S, Fernandes IR, Prado KM, Cardoso EC, Correa-Silva S, Albuquerque R, Knofler M, Beltrao-Braga P, Campa A, Bevilacqua E. The term basal plate of the human placenta as a source of functional extravillous trophoblast cells. *Reprod Biol Endocrinol* 2014; **12**:7.
23. Aplin JD. Expression of integrin alpha 6 beta 4 in human trophoblast and its loss from extravillous cells. *Placenta* 1993; **14**:203–215.
24. Damsky CH, Librach C, Lim KH, Fitzgerald ML, McMaster MT, Janatpour M, Zhou Y, Logan SK, Fisher SJ. Integrin switching regulates normal trophoblast invasion. *Development* 1994; **120**:3657–3666.
25. Vicovac L, Jones CJ, Aplin JD. Trophoblast differentiation during formation of anchoring villi in a model of the early human placenta in vitro. *Placenta* 1995; **16**:41–56.
26. Berx G, Raspe E, Christofori G, Thiery JP, Sleeman JP. Pre-EMTing metastasis? Recapitulation of morphogenetic processes in cancer. *Clin Exp Metastasis* 2007; **24**:587–597.
27. Thiery JP, Acloque H, Huang RY, Nieto MA. Epithelial-mesenchymal transitions in development and disease. *Cell* 2009; **139**:871–890.
28. Lamouille S, Xu J, Derynck R. Molecular mechanisms of epithelial-mesenchymal transition. *Nat Rev Mol Cell Biol* 2014; **15**:178–196.
29. Knofler M. Critical growth factors and signalling pathways controlling human trophoblast invasion. *Int J Dev Biol* 2010; **54**:269–280.
30. Tam WL, Weinberg RA. The epigenetics of epithelial-mesenchymal plasticity in cancer. *Nat Med* 2013; **19**:1438–1449.
31. Ng YH, Zhu H, Leung PC. Twist regulates cadherin-mediated differentiation and fusion of human trophoblastic cells. *J Clin Endocrinol Metab* 2011; **96**:3881–3890.
32. Lu X, He Y, Zhu C, Wang H, Chen S, Lin HY. Twist1 is involved in trophoblast syncytialization by regulating GCM1. *Placenta* 2016; **39**:45–54.
33. Kemp B, Kertschanska S, Kadyrov M, Rath W, Kaufmann P, Huppertz B. Invasive depth of extravillous trophoblast correlates with cellular phenotype: a comparison of intra- and extrauterine implantation sites. *Histochem Cell Biol* 2002; **117**:401–414.
34. Shih JC, Chien CL, Ho HN, Lee WC, Hsieh FJ. Stellate transformation of invasive trophoblast: a distinct phenotype of trophoblast that is involved in decidual vascular remodelling and controlled invasion during pregnancy. *Hum Reprod* 2006; **21**:1299–1304.
35. Peinado H, Olmeda D, Cano A. Snail, Zeb and bHLH factors in tumour progression: an alliance against the epithelial phenotype? *Nat Rev Cancer* 2007; **7**:415–428.
36. Vandewalle C, Comijn J, De Craene B, Vermassen P, Bruyneel E, Andersen H, Tulchinsky E, Van Roy F, Berx G. SIP1/ZEB2 induces EMT by repressing genes of different epithelial cell-cell junctions. *Nucleic Acids Res* 2005; **33**:6566–6578.
37. Onder TT, Gupta PB, Mani SA, Yang J, Lander ES, Weinberg RA. Loss of E-cadherin promotes metastasis via multiple downstream transcriptional pathways. *Cancer Res* 2008; **68**:3645–3654.
38. Bae GY, Choi SJ, Lee JS, Jo J, Lee J, Kim J, Cha HJ. Loss of E-cadherin activates EGFR-MEK/ERK signaling, which promotes invasion via the ZEB1/MMP2 axis in non-small cell lung cancer. *Oncotarget* 2013; **4**:2512–2522.
39. Kocarslan S, Incebiyik A, Guldur ME, Ekinci T, Ozardali HI. What is the role of matrix metalloproteinase-2 in placenta percreta? *J Obstet Gynaecol Res* 2015; **41**:1018–1022.
40. Incebiyik A, Kocarslan S, Camuzcuoglu A, Hilali NG, Incebiyik H, Camuzcuoglu H. Trophoblastic E-cadherin and TGF-beta expression in placenta percreta and normal pregnancies. *J Matern Fetal Neonatal Med* 2016; **29**:126–129.